Charge Homogeneity in Synthetic Fluorohectorite

Josef Breu,*,† Wolfgang Seidl,† Alexander J. Stoll,† Kurt G. Lange,† and Thomas U. Probst‡

Institut für Anorganische Chemie der Universität Regensburg, D-93040 Regensburg, Germany, and Institut für Radiochemie der Technischen Universität München, D-85747 Garching, Germany

Received January 22, 2001. Revised Manuscript Received July 18, 2001

Due to phase separation in the silicate melt, the synthesis of fluorosmectites ($[Na_{0.5}]^{inter}[Mg_{2.5}Li_{0.5}]^{oct}[Si_4]^{tet}O_{10}F_2$) from the melt without mechanical mixing yields an inhomogeneous material. Because of the solid solution capability of the 2:1 layer silicate structure, the nonuniformity in chemical and mineral composition inevitably will lead to fluorosmectites that adopt a range of charge densities. This will be detrimental to many possible applications due to the large influence of layer charge on the properties of clay minerals. The problem can be circumvented by rotating the crucible during synthesis in a horizontal mounting, which will continuously force mixing of the melt mechanically. The product obtained is homogeneous at all length scales as judged by chemical analysis and its uniform intracrystalline reactivity. Noteworthy is its tendency to form regularly interstratified intercalates of monolayers and bilayers upon alkylammonium exchange and of rectorite type phases upon partial K^+ exchange. We expect that the two dissimilar types of galleries, which are stacked in a regularly alternating pattern, can be selectively addressed—leading to interesting intercalation materials.

Introduction

Swelling layered silicates of the 2:1 family with low permanent negative charge (smectites such as montmorillonite, hectorite, etc.; for nomenclature of clay minerals, see Martin et al.[1]) distinguish themselves as 2D host materials because of their rigid, sandwichlike structure built up by two tetrahedral and one octahedral layers (Figure 1a). This lamellar structure is extremely tolerant of substitution and forms solid solutions over a wide range of compositions. Additionally, interlayer cations may easily be altered through cation exchange. Even large inorganic or organic molecules (pillars) may be introduced resulting in microporous or mesoporous pillared clays.[2,3] Due to this variability smectites and their intercalation compounds show a wide range of physicochemical properties. A lot of potential applications, ranging from catalysis,[4−7] nanotechnology,[8,9] adsorption/separation,[10−12] and sensor technology[13] to photofunctions,[14] have been explored over the years.

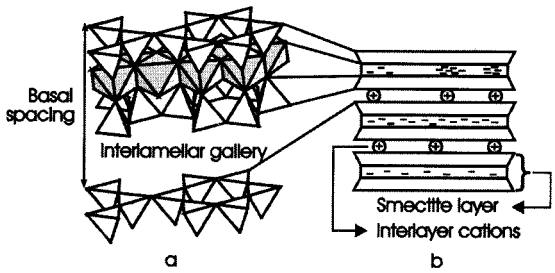

Figure 1. (a) Schematic illustration of the crystal structure of 2:1 layer silicates showing the basal spacing (d_{001}). (b) Schematic representation of an inhomogeneous charge distribution from layer to layer (bottom and middle) and within a single layer (top).

The most important property of smectites is the permanent negative charge density of the silicate layers which manifests itself in the cation-exchange capacity (CEC). With synthetic materials this may, in principle, be tuned over a wide range via the degree of isomorphous substitution of tetrahedral and/or octahedral cations. The resulting CEC in turn determines the density of the cationic pillars introduced after complete cation exchange.

On one hand, the extensive solid solution capability of the 2:1 structure is appealing in terms of the potential

* To whom correspondence should be addressed.
† Universität Regensburg.
‡ Technischen Universität München.

(1) Martin, R. T.; Bailey, S. W.; Eberl, D. D.; Fanning, D. S.; Guggenheim, S.; Kodama, H.; Pevear, D. R.; Srodo'n, J.; Wicks, F. J. *Clays Clay Miner.* **1991**, *39*, 333.
(2) Schoonheydt, R. A.; Pinnavaia, T.; Lagaly, G.; Gangas, N. *Pure Appl. Chem.* **1999**, *71*, 2367.
(3) Gil, A.; Gandia, L. M.; Vicente, M. A. *Catal. Rev.—Sci. Eng.* **2000**, *42*, 145.
(4) Thomas, J. M. *Angew. Chem., Int. Ed. Engl.* **1988**, *27*, 1673.
(5) Breen, C.; Last, P. M. *J. Mater. Chem.* **1999**, *9*, 813.
(6) Cheng, S. *Catal. Today* **1999**, *49*, 303.
(7) Vaccari, A. *Appl. Clay Sci.* **1999**, *14*, 161.
(8) Schöllhorn, R. *Chem. Mater.* **1996**, *8*, 1747.
(9) Lerf, A. Intercalation Compounds in Layered Host Lattices: Supramolecular Chemistry in Nanodimensions. In *Handbook of Nanostructured Materials and Nanotechnology, Vol. 5: Organics, Polymers, and Biological Materials*; Academic Press: San Diego, CA, 2000; p 1.
(10) Boyd, S. A.; Jaynes, W. F. Role of Layer Charge in Organic Contaminant Sorption by Organo-Clays. In *Layer Charge Characteristics of 2:1 Silicate Clay Minerals*; Clay Minerals Society: Boulder, CO, 1994; p 48.
(11) Mercier, L.; Pinnavaia, T. J. *Microporous Mesoporous Mater.* **1998**, *20*, 101.
(12) Barrer, R. M. *Clays Clay Miner.* **1989**, *37*, 385.
(13) Mallouk, T. E.; Gavin, J. A. *Acc. Chem. Res.* **1998**, *31*, 209.
(14) Ogawa, M.; Kuroda, K. *Chem. Rev.* **1995**, *95*, 399.

10.1021/cm011014m CCC: $20.00
Published on Web 10/13/2001

to design new materials with desired properties; see for instance Solin et al.[15] for an inspiring example. On the other hand, it leaves one worrying about the homogeneity of the material synthesized. It has been known that charge densities in natural smectites vary not only from silicate layer to silicate layer in a crystallite[16] but also from domain to domain within a single silicate layer (Figure 1b).[17] Such a heterogeneous distribution of negative charge will of course greatly influence crucial properties of the material—like the distribution of pillars in the interlamellar space.[18]

Therefore, we sought to synthesize a smectite with a perfect uniform distribution of isomorphous substitution. Layer silicates may be synthesized over large ranges of temperature and pressure.[19,20] Among the many approaches described in the literature, synthesis of fluoro analogues from the melt[21] appeared most suitable. Quenching of a homogeneous melt should ensure the best possible homogeneously charged host material. Starting with Johnson[22] and some time later Barrer,[23] the synthesis from the melt of fluoromicas and fluorosmectites with varying compositions has been pursued by many groups over the last 40 years.[15,21,24−30] Largely unnoticed by this clay community, additionally a lot of expertise was gathered in the glass ceramic community, because mica-containing glasses (e.g. Macor, Dicor) show excellent machinablility and mechanical strength.[31−34]

However, there have always been strong hints questioning the homogeneity of these synthetic products.[21,35] For instance, the fact that only part of the interlayer Na^+ may be exchanged in the commercially available synthetic fluoromica from Topy Ind. indicates a nonuniform material.[36]

Since the charge density of the silicate layers is of utmost importance for the properties of the material, we have decided to take a closer look at the uniformity in composition, charge density, and intracrystalline reactivity of a synthetic fluorohectorite.

Experimental Section

Synthesis of Fluorohectorite. The high-purity reagents of SiO_2 (Merck, fine granular, washed and calcined quartz pa), LiF (Aldrich, 99.9%, fused 3−6 mm pieces), MgF_2 (Aldrich, 99.9%, 3−6 mm pieces), MgO (Alfa Aesar, 99.95%, 1−3 fused lumps), and NaF (Aldrich, 99.99%, powder) were carefully weighed out (approximately 0.1 mol) according to the composition corresponding to the formula $[Na_{0.5}]^{inter}[Mg_{2.5}Li_{0.5}]^{oct}[Si_4]^{tet}O_{10}F_2$. NaF cannot be purchased in granular form. Therefore, NaF powder was melted in an open Pt crucible and cast into bullets. The reagents are kept in a glovebox under Argon. The compounds ought to be of high purity and absolutely dry because otherwise the crucible will burst or leak when heated due to evaporation of residual water.

The Mo crucibles (25 mm outer diameter, 21 mm inner diameter, 180 mm overall length) were manufactured by drilling from a rod of pure molybdenum (Plansee, Austria). The crucible was heated in a radio frequency induction furnace applying two differently designed water-cooled coils. While the "reaction-coil" extends over of the full length of the crucible with 22 equally spaced windings, with the "melting-coil" the energy is concentrated by only 4 tight windings in double-layer arrangement to a narrow zone, which allows one to generate temperatures of nearly 3000 °C, enough to melt Mo. To protect the crucible from oxidation at high temperatures it is placed in a quartz tube under high vacuum ($<10^{-4}$ Torr). The quartz tube itself is cooled with a flow of air to prevent crystallization caused by the high heat radiation during synthesis.

Prior to being stocked with reagents, crucible and lid were heated in a vertical position with the reaction-coil to approximately 1600 °C for cleaning purposes. This is necessary to prevent contamination of the sample with carbon, generated by pyrolysis of organic residues from the drilling process. The reagents are then filled into the crucible in an Ar glovebox. Then the crucible is fixed in a water-cooled Cu tube for the next step. To remove residual water adsorbed on the surfaces the upper rim of the crucible is heated to 1200 °C with the melting-coil. At intervals, cooling of the copper tube is interrupted and the temperature in the tube is allowed to rise, improving vaporization of water but at the same time preventing the low-melting fluorides from evaporating. After reaching a sufficient vacuum ($<10^{-4}$ Torr), the now intensively cooled Cu tube is lifted until the slightly conical lid slides into the crucible. After application of short radiation pulses of less than 40 s, the lid is then welded onto the crucible yielding a gastight reaction vessel. Daniels and Moore[37] have reported that fluorine losses by volatilization during melting can be as high as 50% in the synthesis of lithium-containing glass ceramics. Therefore, working in a tightly sealed reaction vessel is crucial.

After sealing, the crucible is placed onto a corundum rod and heated in vertical position with the reaction coil to 2050−2100 °C for a couple of minutes and then kept at 1900 °C for another 20 min. Since the reagents were applied in granular form for purity reasons, for the reaction the maximum temperatures were chosen that can be achieved with quartz tubes for short and prolonged periods, respectively. By switching off the radio frequency, the sample is within seconds quenched to temperatures below 1400 °C, the approximate melting point of the Na−fluorohectorite. To ensure thorough mixing of the melt, the crucible is twice turned upside down and is melted again at 1600−1700 °C for 10 min. This product is referred to in the text as "vertical mounting product".

After the inhomogeneities in composition within the product volume were detected by analysis, yet another synthesis step

(15) Solin, S. A.; Hines, D.; Haushalter, R. *Mol. Cryst. Liq. Cryst. Sci. Technol., Sect. A* **1994**, *244*, 143.
(16) Lagaly, G. Layer Charge Determination by Alkylammonium Ions. In *Layer Charge Characteristics of 2:1 Silicate Clay Minerals*; Clay Minerals Society: Boulder, CO, 1994; p 1.
(17) Muller, F.; Besson, G.; Manceau, A.; Drits, V. A. *Phys. Chem. Miner.* **1997**, *24*, 159.
(18) Breu, J.; Raj, N.; Catlow, C. R. A. *J. Chem. Soc., Dalton Trans.* **1999**, 835.
(19) Grim, R. E. *Clay Mineralogy*; McGraw-Hill: New York, 1968.
(20) Güven, N. Smectites. In *Hydrous Phyllosilicates*; Bailey, G. W., Ed.; Mineralogical Society of America: Washington, DC, 1988; p 497.
(21) Kitajima, K.; Koyama, F.; Takusagawa, N. *Bull. Chem. Soc. Jpn.* **1985**, *58*, 1325.
(22) Johnson, R. C.; Shell, H. R. *Fluorine Mica. R.I. No. 6235*; U.S. Bureau of Mines: Washington, DC, 1963.
(23) Barrer, R. M.; Jones, D. L. *J. Chem. Soc. A* **1970**, 1531.
(24) Takeda, H.; Donnay, G. *Acta Crystallogr.* **1966**, *20*, 638.
(25) Toraya, H.; Iwai, S.; Marumo, F.; Hirao, M. *Z. Kristallogr.* **1977**, *146*, 73.
(26) Toraya, H.; Iwai, S.; Marumo, F.; Daimon, M.; Kondo, R. *Z. Kristallogr.* **1976**, *144*, 42.
(27) Toraya, H.; Iwai, S.; Marumo, F.; Nishikawa, T. *Mineral. J.* **1978**, *9*, 210.
(28) Kitajima, K.; Shinomiya, Y.; Takusagawa, N. *Chem. Lett.* **1984**, 1473.
(29) Kitajima, K.; Ihara, Y.; Takusagawa, N. *J. Ceram. Soc. Jpn.* **1995**, *103*, 1057.
(30) Ihara, Y.; Kitajima, K. *J. Ceram. Soc. Jpn.* **1997**, *105*, 881.
(31) Grossman, D. G. *J. Am. Ceram. Soc.* **1972**, *55*, 446.
(32) Beall, G. H. Structure, Properties, and Applications of Glass-Ceramics. In *Advances in Nucleation and Crystallization in Glasses*; Hench, L. L., Freiman, S. W., Eds.; American Ceramic Society, Inc.: Columbus, OH, 1971; p 251.
(33) Chyung, K.; Beall, G. H.; Grossman, D. G. Fluorophlogopite Mica Glass-Ceramics. In *10th International Congress on Glass, Part II*; Kunughi, M., Tashiro, M., Saga, N., Eds.; The Ceramic Society of Japan: Kyoto, Japan, 1974; p 33.
(34) Hoda, S. N.; Beall, G. H. *Adv. Ceram.* **1982**, *4*, 287.
(35) Miller, J. L.; Johnson, R. C. *Am. Mineral.* **1962**, *47*, 1049.
(36) Soma, M.; Tanaka, A.; Seyama, H.; Hayashi, S.; Hayamizu, K. *Clay Sci.* **1990**, *8*, 1.
(37) Daniels, W. H.; Moore, R. E. *J. Am. Ceram. Soc.* **1975**, *58*, 217.

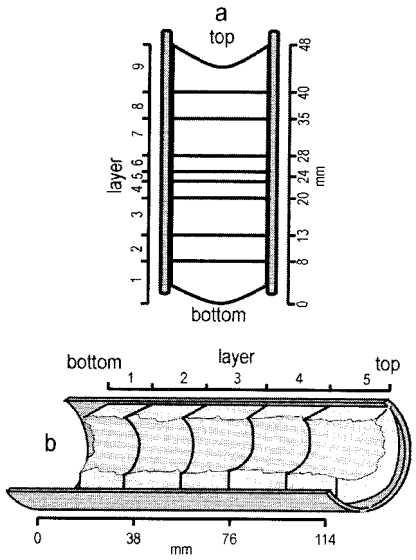

Figure 2. Layering of the (a) "vertical mounting product" and (b) the "horizontal mounting product" for analysis.

was added after the "vertical mounting" reaction. To mechanically minimize gravity segregation in the melt, the crucible in this final step was aligned horizontally and rotated by 60 rpm while heated to 1550 °C for an 1 h and finally to 1650 °C for another 15 min before being quenched by switching off the power supply and flushing the quartz tube with Ar gas. This product is referred to in the text as "horizontal mounting product". If possible, the temperature should of course be raised above the critical temperature. However, the vacuum rotary motion feedthroughs did not allow any higher temperatures for prolonged and short periods, respectively. The quenching rate is approximately the same for "vertical" and "horizontal mounting".

Characterization. The product volume was divided into different layers according to Figure 2. For all layers the chemical composition was determined by wavelength dispersive X-ray fluorescence analysis (WDXRF) which was double checked by inductively coupled plasma atomic emission spectrometry (ICP-AES). For the utmost layers of the "vertical mounting product" there was not enough material available to perform both ICP-AES and RFA.

For partial and total K-exchange 1 g of Na−fluorohectorite was treated for 24 h in a shaker with 40 mL of 0.01 and 0.1 N KCl solutions, respectively. The K/Na ratio for the exchanged materials was determined using an energy dispersive electron microprobe analyzer (Link QX 200).

Quantitative alkylammonium exchange was achieved using literature procedures.[16,38] The amines ($C_nH_{2n+1}NH_2$; $n = 7-12$) were purchased from Aldrich and converted to formiates by neutralization with formic acid.[16]

Chemical Analysis. WDXRF. Analyses were performed with borate glass disks (1.25 g of sample + 5 g of Spectroflux SF110A, Johnson Matthey Chemicals Ltd.) on a Philips PW 1400 spectrometer, which was calibrated applying international rock standards.

ICP-AES. The 100 mg samples were weighed into precleaned Teflon vessels of 150 mL volume. After addition of 1.5 mL of 30% v/v HCl (Merck, suprapur), 0.5 mL of 65% v/v HNO_3, 0.4 mL of 40% v/v HF (Merck, suprapur), and 8 mL of 2% w/w H_3BO_3 (Merck, pa), the samples were digested in a MLS 1200 Mega microwave digestion apparatus (MLS GmbH, Mikrowellen-Labor-Systeme, Leutkirch, Germany) for a total of 31.5 min. The microwave program consisted of 10 min of heating at 300 W, 5 min of ventilation, 6.5 min of heating at 600 W, and again 10 min of ventilation. The closed sample containers were cooled within 1 h to room temperature. The obtained homogeneous solutions were diluted 1:10 with a mixture of 1 M HNO_3 and 0.1 M H_3BO_3. Reference digestions for the control of Si amounts were performed by digestion of a reference glass standard (BCS-CRM 313/1).

Table 1. ICP-AES Operating Conditions

ICP system		emissions spectrometer	
sample uptake (mL/min)	1.1	wavelength (nm)	
washing time (s)	160	Li	670.784, 610.362
plasma power (W)	1083	Mg	279.553, 280.270
Ar flow rates		Na	588.995, 589.592
nebulizer (L/min)	2	Rh	246.104, 251.103
auxiliary (L/min)	0.945	Ru	240.272, 267.876
plasma (L/min)	15	Si	251.611, 212.412

A sequentially operating ICP-AES plasma emission spectrometer Plasma 40/400 of Perkin-Elmer (Überlingen, Germany) equipped with a Ryton spray chamber, a quartz injector tube in the Fassel torch, and an autosampler AS-90 (Perkin-Elmer) were employed for the analysis of Li, Mg, Na, Ru, and Si. Rhodium in a concentration of 10 μg/mL was used as an internal standard. Element standards were prepared by weight-controlled dilutions of 1000 μg/mL AAS standard solutions of the individual elements by a mixture of 1 M HNO_3 and 0.1 M H_3BO_3.

The operating conditions are summarized in Table 1.

X-ray Diffraction. X-ray Diffraction (XRD) patterns of the Na−fluorohectorite were obtained in transmission mode on a Stoe Stadi powder diffractometer. To minimize texture the samples were placed in Lindemann glass capillaries. The alkylammonium-exchanged samples were measured on the same diffractometer but on flat sample holders. The textured samples of the hydrated phases were prepared on glass slides by sedimentation. A 100% humidity was achieved by carefully spraying water on the textured samples immediately before recording the diffraction traces in Bragg−Brentano geometry on a Siemens D 5000. Both diffractometers were equipped with monochromators, and Cu Kα radiation was used.

Results and Discussion

The microcrystalline product obtained in "vertical mounting" showed slightly gray opalescence and appeared optically homogeneous. Crystallites were radially interlocked to a hard conglomerate. This Na−fluorohectorite spontaneously absorbs water ($\approx$2 H_2O/formula unit) from the air to form a monolayer−hydrate (d = 12.4 Å), and the regulus falls apart. The particle size distribution of the synthetic Na−fluorohectorite shows a maximum at approximately 9 μm, clearly shifted to larger particles as compared to natural smectites. This is also resembled by the much narrower 00*l* reflections indicating much thicker crystallites along the stacking direction (Figure 3). As observed by others before,[21,23] the Na−fluorohectorite contained minor impurities of protoamphibole, an orthorhombic fluoroamphibole.[39] Because of the similarity of building blocks the amphibole structure appears to be a natural competitor for the 2:1 layer structure. However, the amphibole structure is slightly denser. By use of Toraya's taeniolite cell[25] but adjusted for the lower basal spacing observed for the synthesized Na−fluorohectorite and in combination with the cell content given by the ideal anhydrous composition, a density of 2.806 g cm^{-3} will result for the Na−fluorohectorite. Gibbs et al.[39] found 2.928 g cm^{-3} for a typical protoamphibole with a composition of $Na_{0.05}Li_{1.12}Mg_{6.52}Si_{7.93}O_{21.91}F_{2.09}$.

(38) Lagaly, G. *Clay Miner.* **1981**, *16*, 1.

(39) Gibbs, G. V.; Bloss, F. D.; Shell, H. R. *Am. Mineral.* **1960**, *45*, 974.

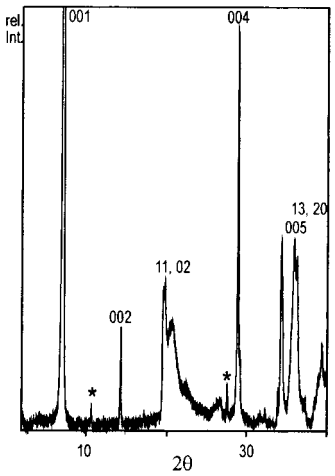

Figure 3. Diffraction profiles of the 1-layer hydrate of the synthetic Na−fluorohectorite. The strongest protoamphibole peaks are marked with asterisks. Three indices indicate basal reflections; two indices indicate 2D *hk* bands.

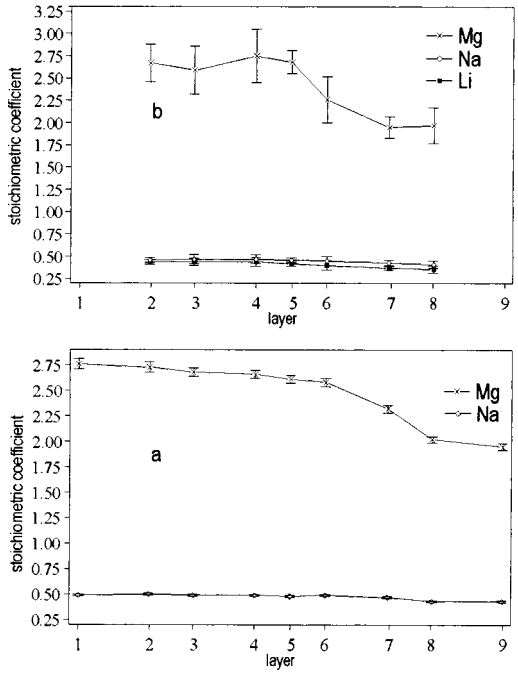

Figure 4. Results of chemical analysis by (a) WDXRF and (b) ICP-AES for the "vertical mounting product". Stoichiometric coefficients are normalized to $Si_{4.0}$.

Chemical and XRD Analysis. To our great surprise, when the homogeneity of the product body was checked, a clear drift in composition becomes obvious (Figure 4). Repeated flipping of the Mo vessel with subsequent remelting did not alter the picture suggesting that the drift was not caused by insufficient mixing of the reagents but rather is system immanent. WDXRF and ICP-AES results in agreement show a significant depletion of Mg contents in the top of the product volume. Moreover, this nonuniformity in chemical composition also manifested itself in varying protoamphibole contents (Figure 5). As judged by the intensity of the 110 and 131 peaks of protoamphibole, the concentration of this secondary product is highest in the middle of the product volume. The protoamphibole concentration does follow the drift in composition inasmuch as it sharply

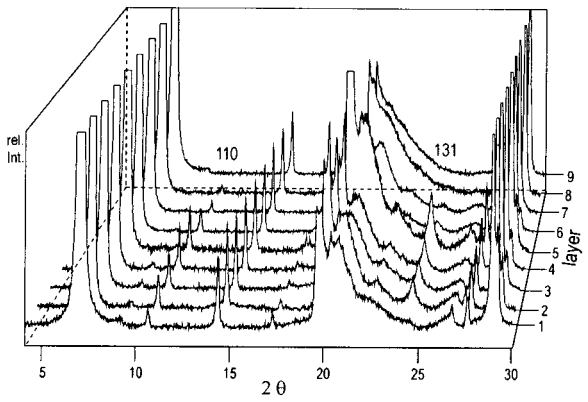

Figure 5. XRD profiles for the different layers of the anhydrous "vertical mounting product". The strongest protoamphibole peaks are indexed.

falls off with decreasing Mg content at the top. However, it also decreases at the bottom of the regulus. Apparently, protoamphibole production is not only influenced by the composition but also by the cooling rate which will be higher at the ends of the crucible. Most likely, such inhomogeneities are system immanent but have escaped detection in previously reported studies because analysis was not performed with spatial resolution. Clearly, the implications of this nonuniformity in chemical and mineral composition are that fluorosmectites synthesized from the melt without any precaution in a "vertical mounting" inevitably will adopt a range of charge densities. This will be detrimental to many possible applications, because of the large influence of the layer charge on properties of 2:1 clay minerals.

What could be causing this problem? The equilibrium of the homogeneous melt is destroyed in many composite systems by separation into two liquid phases. Many glass-forming melts exhibit a miscibility gap, which is only closed above a certain critical temperature.[40] Phase diagrams and miscibility gaps of such complicated mixtures as applied in the fluorohectorite synthesis have not yet been determined. However, it is known that among the pseudobinary alkali metal and alkaline earth silicate systems the $MgO-SiO_2$ system displays the highest critical temperature (>2000 °C; see ref 41 for a phase diagram) which even increases upon addition of fluorine.[42] Therefore, it is reasonable to assume that we will have to deal with phase separation into two liquid phases with different composition. Further, if one presumes that the density difference of the two liquid phases resembles that found in the resulting crystalline phases, then the inhomogeneities observed in the product volume might very well be induced by gravity driven segregation in the melt.

Since phase separation can be a spontaneous (spinodal) process, even raising the synthesis temperature above the critical temperature and high cooling rates will not necessarily prevent separation into two liquid phases interpenetrating each other. Therefore, we rather pursued the finest possible dispersion of the two liquid

(40) Feltz, A. *Amorphous Inorganic Materials and Glasses*; VCH: Weinheim, Germany, 1993.
(41) McGahay, V.; Tomozawa, M. *J. Non-Cryst. Solids* **1989**, *109*, 27.
(42) Markis, J. H.; Clemens, K.; Tomozawa, M. *J. Am. Ceram. Soc.* **1981**, *64*, C-20.

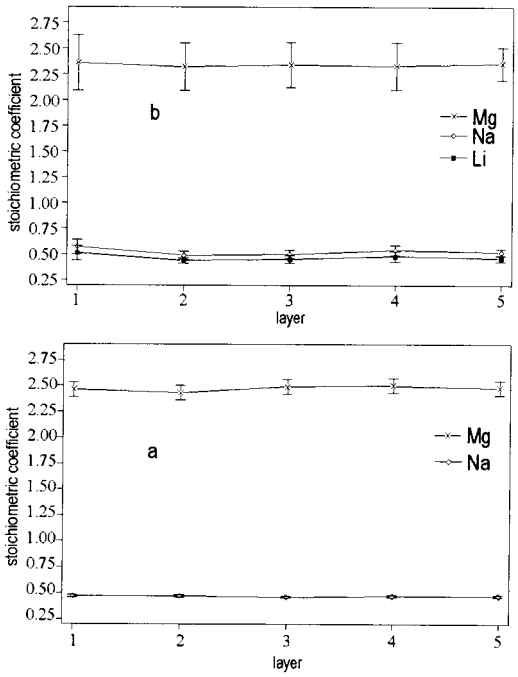

Figure 6. Results of chemical analysis by (a) WDXRF and (b) ICP-AES for the "horizontal mounting product". Stoichiometric coefficients are normalized to $Si_{4.0}$.

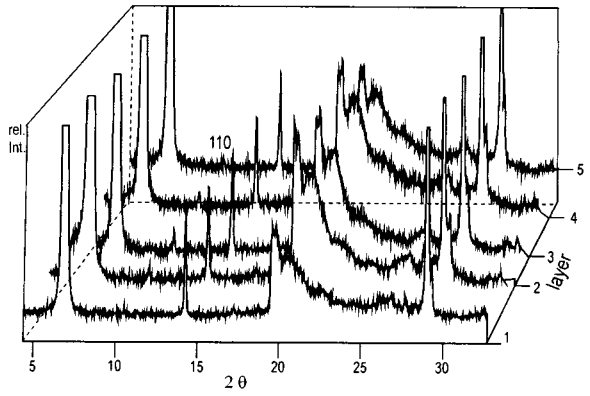

Figure 7. XRD profiles for the different layers of the anhydrous "horizontal mounting product". The strongest protoamphibole peaks are indexed.

phases by rotating the crucible in a horizontal position, which will continuously force mixing of the melt mechanically.

The analysis results of this "horizontal mounting product" are convincing (Figure 6 and Figure 7). The chemical composition is uniform over the whole product volume and corresponds to the desired stoichiometry. Even more pleasing is the fact that the secondary phase is considerably reduced. Protoamphibole is now only present in traces close to the detection limit.

Intracrystalline Reactivity. *Swelling with Water.* The analysis results still do not ensure a uniform charge density at the smaller length scales. The homogeneity at the level of different crystallites shall be judged on the intracrystalline reactivity toward water. Swelling natural 2:1 layer silicates with homoionic interlayer cations realize distinct hydration levels depending on the relative humidity. For Na−smectites four hydration states are known that show basal spacings of 10.0, 12.4, 15.6, and 18.8 Å, corresponding to 0, 1, 2, and 3 layers

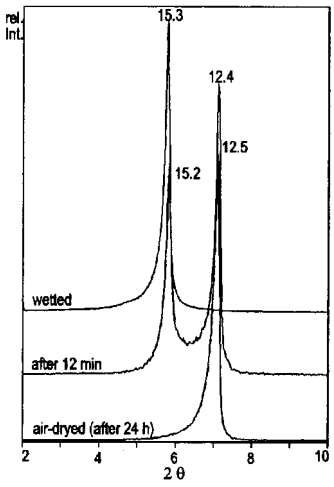

Figure 8. Evolution of XRD profiles during dehydration of the 2-layer hydrate of the synthetic Na−fluorohectorite (basal spacings in Å).

of water molecules, respectively. However, particularly in natural smectites with their nonuniform charge density individual interlayers within one crystallite may adopt different hydration levels at the same vapor pressure. For these randomly interstratified structures irrational 00*l* series are observed with apparent basal spacings between the above values.

Kitajima[21] reported another kind of nonuniform swelling behavior for his synthetic Na−fluorohectorite. He observed two distinct basal spacings and hence hydration levels at the same time. This indicates that individual crystallites (or at least domains larger than the coherence lengths of the X-rays) realize distinct hydration levels, which most likely is caused by different charge density levels of these crystallites.

We covered textured samples of the synthesized Na−fluorohectorite with a thin film of water and followed the dynamics of interlayer water loss (Figure 8). At 100% humidity a 2-layer hydrate is formed, and at ambient relative humidity (50−60%) a 1-layer hydrate is formed. At a given vapor pressure all crystallites accomplish the same hydration level. Moreover, at any time during the drying period these are the only hydration stages observed. This implies that individual interlayers within a crystallite lose the second layer of water at the same time in a cooperative manner. This uniform swelling behavior is taken as a strong indication for a homogeneous charge density.

Cation Exchange with Potassium Ions. Unlike what has been reported for the Na−fluorotaeniolithe from Topy Ind., where only 60% of the Na^+ ions can be exchanged,[36] with the synthetic fluorohectorite a quantitative exchange of interlayer cations for K^+ is possible (Figure 9) and an integral 00*l* series with a basal spacing of 10.1 Å is observed. This implies that upon potassium exchange the interlayers dehydrate and collapse. Interestingly, at partial exchange a tendency for a segregation of the two inorganic cations into different interlayers is observed. Moreover, the dehydrated K interlayers and the hydrated Na interlayers tend to form a regular interstratification. In Figure 9 the situation with a K/Na ratio of 1.86 (determined by energy dispersive electron microprobe analysis) is depicted. Besides the basal spacing of the 1-layer hydrate

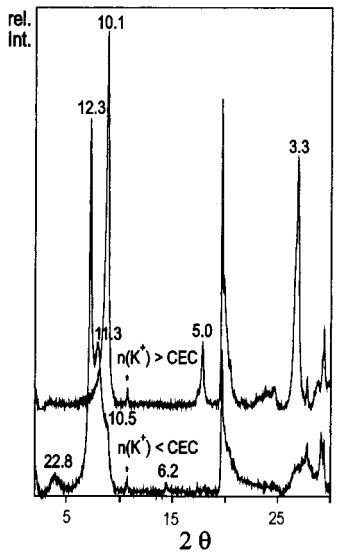

Figure 9. XRD profiles of partially ($n(K^+)$ < CEC) and quantitatively ($n(K^+)$ > CEC) K^+-exchanged synthetic Na−fluorohectorite (basal spacings in Å).

at d = 12.3 Å and a shoulder at the position of the dehydrated K−fluorohectorite ($d \approx 10$ Å), basal reflections of the ordered *superstructure* can be observed (d = 22.8 Å, d = 11.3 Å). Interestingly, with our synthetic fluorohectorite these rectorite-like analogues are spontaneously created by a simple partial ion exchange, while Ijdo et al.[43] had to take the detour via tetraalkylphosphonium and -ammonium derivatives to obtain these regularly alternating pattern of different galleries.

This cation exchange behavior resembles what has been observed for Na−taeniolite upon K^+ exchange[44] and for a synthetic Na−fluorovermiculite upon Mg^{2+} exchange.[45] However, in both these cases a considerable amount of Na^+ was nonexchangeable.

Tateyama et al.[45] rationalized this regular interstratification by assuming a different degree of isomorphous substitution in the two tetrahedral sheets composing a silicate layer as has been discussed before for rectorite, a natural regularly interstratified clay.[46] The resulting polar silicate layers are supposed to be arranged in such a way as to give rise to alternating low and high charge density interlayers. However, since the permanent charge in hectorites results from an isomorphous substitution in the octahedral sheet, the silicate layers cannot adopt a polar structure. Thus, this rationale can be excluded for our material. We rather favor an explanation given for vermiculites, where K^+ sorption also causes collapse of alternate interlayers producing regularly interstratified materials.[47] Sawhney hypothesized that collapse in one layer of vermiculite on K^+ sorption reduces the interlayer cation density of the adjacent interlayers. In other words, on collapse more K^+ is trapped in that interlayer than the average cation density corresponding to layer charges of the adjacent silicate layer would require. For nonpolar silicate layers this is energetically feasible since the charge balance is equally "local" for the two cases of a 50/50 or a 25/75 distribution of the counter charge in the interlamellar space above/below, respectively. As a consequence of the higher cation density in the collapsed K interlayers, the bonding energy of K^+ to the silicate in the adjacent interlayers is smaller than the hydration energy of the Na^+ ions; hence, K^+ would not enter this interlayer but would enter the next interlayer, producing a regularly interstratified mixed layer material. The mechanism would of course break down should the charge density of the silicate layers vary considerably along the stacking direction. This view is in line with the fact that with natural smectites, which are known to have a heterogeneous charge density, collapse occurs randomly. The regular interstratification upon cation exchange is only observed with vermiculites that generally display a much less pronounced charge heterogeneity as compared to natural smectites.

In summary, the experimental observations upon cation exchange with K^+ again strongly indicate a homogeneous charge distribution in the synthesized Na−fluorohectorite.

Cation Exchange with Alkylammonium Ions. As a final test on charge density homogeneity within the "horizontal mounting product" a layer charge determination according to Lagaly and Weiss was attempted. This method estimates the interlayer cation density by measuring the basal spacing of a complete series of alkylammonium derivatives ($C_nH_{2n+1}NH_3^+HCO_2^-$; n = 4−9). The alkylammonium ions displace the interlayer cations quantitatively. Depending on the charge density and the length of the alkylchain, the alkylammonium ions in the interlayer space are arranged in different structures. If the cation density is < 0.5 as with smectites, the alkylammonium ions are organized in structures with flat lying chains parallel to the silicate layers. With small chain lengths monolayers will be realized with a characteristic integral basal reflection at 13.4−13.6 Å. With increase of n, at some point these monolayers will be closely packed. With the next chain length applied, bilayers with a basal spacing of typically 17.6 Å are needed to satisfy the charge density of the host. The minimum charge density of the host can be deduced from the area demand of the last alkylammonium ion that is able to realize charge neutrality with a monolayer. The area of an alkylammonium ion can be estimated to be $1.27 \times 4.5 \times n + 14$ (Å^2).[48] Assuming the same unit cell for the fluorohectorite as determined for taeniolite[25] (ab = 47.4 Å^2), the critical chain length expected for a layer charge of x = 0.5 will be n = 5. Starting with n = 6, the charge density can only be satisfied by realizing some bilayers. Note that since n is an integer with this method only the limits of the charge density can be given.

For natural smectites the transition from the monolayer to the bilayer plateau is not sharp but instead a smooth transition for a range of intermediate chain lengths n is observed. Furthermore, for natural smectites the pronounced nonintegrality of basal reflections indicates a random interstratification of differently expanded interlayer spaces. This is explained by the

(43) Ijdo, W. L.; Lee, T.; Pinnavaia, T. J. *Adv. Mater.* **1996**, *8*, 79.
(44) Miyake, M.; Suzuki, T. *Chem. Mater.* **1993**, *5*, 1327.
(45) Tateyama, H.; Noma, H.; Nishimura, S.; Adachi, Y.; Ooi, M.; Urabe, K. *Clays Clay Miner.* **1998**, *46*, 245.
(46) Brown, G. *Philos. Trans. R. Soc. London, Ser. A* **1984**, *311*, 221.
(47) Sawhney, B. L. *Clays Clay Miner.* **1972**, *20*, 93.
(48) Lagaly, G.; Weiss, A. *Kolloid Z. Z. Polym.* **1971**, *243*, 48.

heterogeneity of charge densities in natural smectites.[16] Such transitional chain lengths will still realize some monolayers for interlayers with lower cation density while more highly charged interlayers already have to reside to bilayers at the given *n*. The crystal is composed of 13.4 and 17.6 Å layers in a random sequence. The ratio between these two will increase with *n*, and the observed basal spacing, averaged by the X-rays, will migrate over the transition range until eventually only bilayers are present giving rise to sharp integral 00*l* reflections again. With the help of charge migration curves the migration of the basal peak can be translated into a charge distribution histogram (see Lagaly for examples[16,38]).

The picture observed with our synthetic Na−fluorohectorite upon alkylammonium exchange is rather different from what has been observed with natural smectites. Quite surprisingly, instead of a random we observe a regular interstratification giving rise to a *superstructure* reflection at approximately 31 Å (Figure 10a).

A complete description of these mixed-layer intercalation compounds requires not only the identification of the types of layers involved but also the proportions of each and the type of order or lack thereof in the stacking sequence of monolayers and bilayers along the *z* direction (*Reichweite, R*). A perfectly ordered mixed-layer material that gives rise to a rational series of 00*l* reflections of the superstrucutre requires not only *R*1 but also equal molecular proportions (existence probabilities). If the proportions of the two types of layers are not equal, a certain degree of randomness must occur in the stacking even with *R*1 (see ref 49, p 174f). Irrationality of 00*l* diffraction patterns will evidence this randomness in the interstratification. As with random interstratification, the observed reflections will then be compromises of the nominal positions of the two layer types in the mixture. The maximum is broad if end-member reflections are far apart and sharp if they are close together. Thus, not only the position and intensity of the basal reflections are of diagnostic value but also the shape of the peaks. For a complete analysis the parameters Reichweite and existence probability would have to be varied in trial and error calculations of XRD profiles utilizing e.g. NEWMOD.[50] Then the calculated diffraction profiles would have to be compared with the experimental traces.[45,51] Such a detailed analysis is beyond the scope of this paper; only a qualitative discussion will be presented.

As expected from charge density considerations up to $n = 5$, the alkylammonium ions are arranged in a monolayer. According to Lagaly[16] an upper limit of the charge density of 0.56 may be deduced from this. With $n = 6-8$ the *superstructure* reflection observed at approximately 31 Å is indicating a nonrandom interstratification of monolayers and bilayers. While Ijdo et al. were able to synthesize ordered structures with two

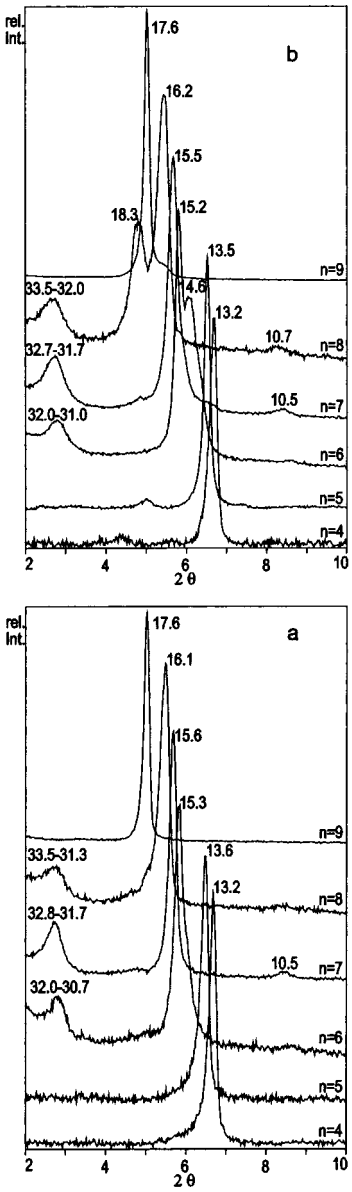

Figure 10. Evolution of XRD profiles with increasing chain length (*n*) upon akylammonium exchange for (a) layer 5 and (b) layer 3 of the "horizontal mounting product". Note the *superstructure* reflections at intermediate chain lengths (basal spacings in Å).

different kinds of organocations[43] or mixed organic−inorganic interlayers,[52] this is the first time that, to our knowledge, an ordered interstratification is observed with a homoionic organoclay.

Again, this strong tendency for a regular interstratification may be interpreted as an indication for a perfect homogeneous charge density in consecutive interlayers. Why should a regular interstratification of monolayers and bilayers be energetically preferred in homogeneously charged smectites? As outlined above, since the origin of the permanent negative charge density is at the center of the silicate layer, charge balance is equally "local" for different proportions of charge balance above and below the layer. Additionally, with *n* being too large to satisfy the charge density of the host in a monolayer, a uniform distribution of the alkylammonium ions over

(49) Moore, D. M.; Reynolds, R. C. J. *X-ray Diffraction and the Identification and Analysis of Clay Minerals*; Oxford University Press: Oxford, U.K., 1997.

(50) Walker, J. R. An Introduction to Computer Modeling of X-ray Diffraction Patterns of Clay Minerals: A Guided Tour of NEWMOD. In *Computer Applications to X-ray Powder Diffraction Analysis of Clay Minerals*; The Clay Mineral Society: Boulder, CO, 1993; p 1.

(51) Roberson, H. E.; Reynolds, R. C.; Jenkins, D. M. *Clays Clay Miner.* **1999**, *47*, 212.

(52) Ijdo, W. L.; Pinnavaia, T. J. *Chem. Mater.* **1999**, *11*, 3227.

all the interlayers would require that at one hand all interlayers are expanded to a bilayer basal spacing against the Coulombic attraction. At the other hand, the alkylammonium ions needed for charge balance would then be too few to yield a dense packing of the interlamellar space. Contrary to this, segregation of counterions into interlayers with monolayers and bilayers of alkylammonium ions allows a dense packing of the interlamellar space and at the same time only a minimum of interlayers have to be expanded. Overall charge balance can easily be adjusted by varying the existence probabilities of monolayers and bilayers. Assuming the same charge density in each interlayer and accepting that the alkylammonium ions always form closed-packed bilayers, the driving force for a perfect *R*1 type ordering is the preference for a "local" balance of the uniform permanent negative charge of the silicate layers. Moreover, this view is indeed in line with further experimental observations. As outlined above, the series of 00*l* superstructure reflections cannot be rational because the existence probabilities of monolayers and bilayers are determined by the charge of the smectite and therefore in general will not be equal. However, it is expected that with increasing chain length the existence probability of close packed bilayers will have to increase. For a perfectly ordered structure (equal existence probability and *R*1) the 002 reflection of the superstructure is expected at $d = 15.6$ Å (0.5 × (13.6 Å + 17.6 Å)). A value larger than this indicates a surplus of bilayers, and a smaller value, a surplus of monolayers. The basal spacings observed (layer 5) are 15.3, 15.6, and 16.1 Å for *n* equal to 6, 7, and 8, respectively, which is in line with the expected trend. Moreover, with the medium chain length, which according to the observed *d* value is expected to be closest to a 50/50 composition, the reflections are sharper and even the 003 interference of the *superstructure* is observed.

Beside the above-mentioned thermodynamic reasons, regularly interstratified structures might also be caused by kinetics. As outlined in some detail by Lagaly,[53] when the inorganic interlayer cations are replaced by larger organic cations in any arbitrary interlayer space, the concomitant opening of the interlayer space will bend the silicate layers toward the adjacent interlayers. In a negative cooperativity this may obstruct the reaction in the two adjacent interlayers. If the charge density in the reacting layer cannot be satisfied by a monolayer, even bilayers may be formed before the first organic cations are able to enter the adjacent interlayers. In combination with the irreversible nature of the cation exchange this would also lead to regularly interstratified materials.

It is worth pointing out that even within this very homogeneous fluorohectorite, the alkylammonium method is capable of revealing small differences in the layer charge and charge distribution. Intracrystalline reactivities in the different product layers are very similar but not totally identical. In a comparison of the diffractogramms of the so far discussed layer 5 (Figure 10a) with the central layer 3 (Figure 10b), small differences become apparent. The discussion will be limited to these two representative layers from the periphery and the center. While the XRD traces in layer 5 in the mixed layer region ($n = 6-8$) only contain peaks that belong to an ordered (*R*1) superstructure, in layer 3 additional peaks are observed that can be assigned to a more randomly mixed layer material. With $n = 6$ an additional maximum at 14.6 Å is visible that indicates a random interstratification of bilayers with monolayers. With $n = 8$ a reflection at 18.3 Å shows that apart from the mixed layer material domains of pure bilayers are present.

Finally, we note that the pronounced tendency of the synthetic fluorohectorite to gallery segregation is not only fundamentally interesting from a structural viewpoint but may also prove to be leading to novel materials with interesting properties. In principle, the two dissimilar types of galleries which are stacked in a regularly alternating pattern can be selectively addressed[43] and altered using all kinds of established intercalation reactions. For instance, a range of hybrid organic–inorganic composites with tuneable properties will be accessible.[52] By combination of the hydrophobic and hydrophilic properties of mixed layer materials containing organic and inorganic interlayers, respectively, amphiphilic materials result that might find applications as versatile ion exchangers, sorbents, and nanoparticle reagents. Also, a photosensitizer in one interlayer space may be separated from reagents located in the adjacent interlayers.

Acknowledgment. We are grateful to the DFG and the Fonds der Chemischen Industrie for financial support.

CM011014M

(53) Lagaly, G. Smectitic Clays as Ionic Macromolecules. In *Developments in Ionic Polymers*; Elsevier: London, 1986; p 77.